



UNIVERSITÀ
DEGLI STUDI
FIRENZE

FLORE

Repository istituzionale dell'Università degli Studi di Firenze

Exergoeconomic analysis and comparison between ORC and Kalina cycles to exploit low and medium-high temperature heat from two

Questa è la versione Preprint (Submitted version) della seguente pubblicazione:

Original Citation:

Exergoeconomic analysis and comparison between ORC and Kalina cycles to exploit low and medium-high temperature heat from two different geothermal sites / Fiaschi, Daniele; Manfrida, Giampaolo; Rogai, E.; Talluri, Lorenzo. - In: ENERGY CONVERSION AND MANAGEMENT. - ISSN 0196-8904. - ELETTRONICO. - 154:(2017), pp. 503-516. [10.1016/j.enconman.2017.11.034]

Availability:

The webpage <https://hdl.handle.net/2158/1104182> of the repository was last updated on 2021-04-09T11:53:56Z

Published version:

DOI: 10.1016/j.enconman.2017.11.034

Terms of use:

Open Access

La pubblicazione è resa disponibile sotto le norme e i termini della licenza di deposito, secondo quanto stabilito dalla Policy per l'accesso aperto dell'Università degli Studi di Firenze (<https://www.sba.unifi.it/upload/policy-oa-2016-1.pdf>)

Publisher copyright claim:

Conformità alle politiche dell'editore / Compliance to publisher's policies

Questa versione della pubblicazione è conforme a quanto richiesto dalle politiche dell'editore in materia di copyright.

This version of the publication conforms to the publisher's copyright policies.

La data sopra indicata si riferisce all'ultimo aggiornamento della scheda del Repository FloRe - The above-mentioned date refers to the last update of the record in the Institutional Repository FloRe

(Article begins on next page)

1 **Exergo economic analysis and comparison between ORC and Kalina cycles to exploit low and medium-high**
2 **temperature heat from two different geothermal sites**

3
4 *D. Fiaschi^a, G. Manfrida^a, E. Rogai^a, L. Talluri^a;

5 ^aDepartment of Industrial Engineering, University of Florence, Florence, Viale Morgagni 40-44, 50134, Italy

6 *Corresponding author

7
8 **KEYWORDS**

9 Geothermal energy, binary cycle, Kalina, ORC, Exergo Economic, Electricity production cost

10
11
12 **Abstract (240 words)**

13 The Organic Rankine (ORC) and Kalina (KC) Cycles represent two different technologies suitable to exploit low and
14 medium temperature geothermal heat resources. In this work, the performances of KC, CO₂ and ORC cycles, the latter
15 using different working fluids, for power generation from two geothermal fluid reservoirs are compared from an energy
16 and exergo-economic perspective.

17 Two different case studies are discussed: the first one referred to a medium-temperature heat source of 212 °C (Mt.
18 Amiata, Italy), the second one to a low-temperature heat source of 120 °C (Pomarance geothermal basin, Italy).

19 For each case study, cost rate balances and auxiliary equations for all components were evaluated, as well as the flow
20 rate and unit exergy cost for each stream.

21 The results for the medium temperature case study showed that, among the considered cycles, an ORC with
22 R1233zd(E) achieves the best exergoeconomic performance. The cost of the produced electricity was found to be 8.85
23 c€/kWh, which is 3% lower than that of the KC. On the other hand, for the low temperature case study, the KC shows
24 the best performance, being able to produce 22 – 42% more net power than the ORC; in this case, the cost of electricity
25 produced by the KC was found at 12.5 c€/kWh, which is 24-34% lower than the typical value for an ORC with different
26 working fluids.

27

28

*Corresponding author. **Tel.:** +39 055 2758680, **E-mail address:** daniele.fiaschi@unifi.it

29 NOMENCLATURE

Symbols

c_{jk}, c_{ik}	Flux costs, [€/kJ]
$cost_{fuel_{kj}}$	Geothermal fluid specific exergy cost, [€/kJ]
$cost_{Wt_{kj}}$	Turbine power specific cost, [€/kJ]
$cost_{kWh_{el}}$	Produced kWh cost, $\left[\frac{c\text{€}}{kWh}\right]$
\dot{C}_P	Output product cost, [€/s]
\dot{C}_F	Fuel cost, [€/s]
ex	Specific exergy, [kJ/kg]
f	Exergo-economic factor
h	Enthalpy, [kJ/kg]
i_{eff}	Effective interest rate
n	Power plant lifespan (yr)
P	Pressure, [Pa, bar]
Q	Thermal power, [kW]
R	Heat resistance, [K/W]
s	Entropy, [kJ/kg-K]
T	Temperature [K, °C]
\dot{Z}	Capital Investment
x	Ammonia mass fraction [-]
W	Power, [kW]

\dot{m} Mass flow rate, [kg/s]

Greek symbols

η	First law efficiency, [-]
η_{II}	Second law efficiency, [-]
ρ	Density, [kg m ⁻²]

Subscripts

0	Reference state
1, 2, 3, ...	Cycle reference points
base fluid	Ammonia water mixture before separator
Geo	Geothermal fluid
in/out	Inlet/Outlet

Acronyms

CEPCI	Chemical Engineering Plant Cost Index
EES	Engineering Equation Solver
KC	Kalina Cycle
PEC	Purchased equipment costs
TCI	Total Capital Investment

31 **1. Introduction**

32 In recent years, an increasing interest towards the exploitation of low temperature heat to produce electricity, both from
33 renewables and industrial wastes, is coming out. Among renewables, geothermal energy presents the highest
34 availability, as it does not substantially depend on weather conditions. Nowadays, the technology for the electricity
35 conversion of geothermal energy achieved a wide market application, with over 10,000 MWe installed. However, the
36 exploitation of conventional resources (high- and mediumtemperature) almost reached its maximum potential, and the
37 not yet utilized fields are often at low or moderate temperature. On the other hand, there is a growing interest towards
38 the exploitation of low temperature geothermal resources to produce electricity. Anyhow, it is a challenging task due to
39 thermodynamic, environmental and economic issues; conventional conversion methods, indeed, do not guarantee viable
40 solutions.

41 The environmental sustainability of geothermal energy conversion systems was deeply addressed employing life cycle
42 analysis as an evaluation tool (Bayer et. al, 2013, Bravi and Basosi, 2014, Frick et. al., 2013, Saner et. al., 2010). A
43 relevant documented issue is the release of non-condensable gases to the environment, containing several kinds of
44 contaminants. Only the use of binary cycles (like ORCs or Kalina) coupled to the complete reinjection of non –
45 condensable gases could give a valuable answer to the improvement of sustainability of geothermal power plants, as
46 demonstrated in (Bravi and Basosi, 2014, Frick, S., et. al., 2013, Saner et. al., 2010). These cycles, also working with
47 novel and environmentally friendly fluids (low GWP) are a pivotal point for the exploitation of low temperature
48 geothermal resources.

49 Recently, numerous studies on the assessment of ORC as geothermal energy conversion systems (Zeyghami, 2015;
50 Walraven et al., 2015), including optimal working fluids selection (Liu e al., 2013) and zeotropic mixtures (Liu et al.,
51 2014).were carried out.

52 A very efficient configuration of geothermal conversion system is the combined heat and power arrangements, which
53 allows a decisive enhancement of net plant efficiency (Fiaschi et al., 2014). Another interesting way to enhance ORC
54 geothermal plant efficiencies is to consider supercritical configuration power plants (Arslan and Yetik, 2011).

55 Another technology, which holds high efficiency for low temperature resources, is the Kalina cycle (KC), based on an
56 ammonia-water mixture as working fluid in place of a pure substance. In the early eighties of the twentieth century,
57 Alexander I. Kalina proposed this new thermodynamic cycle (Kalina, 1982). Among the advanced thermodynamic
58 cycles, KC is the most significant improvement in energy systems design since the advent of the Rankine cycle in the
59 mid of the 19th century, and is acknowledged to be an ambitious competitor of the ORC (Zhang, 2012). The main trait
60 of non-azeotropic mixtures, such as the ammonia-water mixture, is the transition phase at variable temperature during

61 vaporization and condensation. This peculiarity allows a better coupling between the heat capacities of the fluids in both
62 evaporator and condenser, thus reducing the irreversibilities due to the heat transfer and, therefore, enhancing the
63 overall efficiency of the system (Valdimarsson, 2003).

64 Many parametric studies were carried out on the performance evaluation of KC with ammonia-water mixture for the
65 exploitation of low temperature heat resources, also including exergy analysis (Ibrahim and Kovach, 1993, Nag and
66 Gupta, 1997). It was found that the increase of the ammonia mass fraction would hold positive effects on the turbine
67 losses, while increasing the evaporator losses. This trend is due to better matching of the thermal profiles between the
68 heat source and the working fluid, allowing a reduction of irreversibility at the evaporator when the ammonia mass
69 fraction is lower. Fiaschi et. al. (2015) investigated a new configuration of KC for low temperature geothermal
70 resources including a chiller, thus making the power cycle a cold cogeneration and power unit by exploiting the
71 properties of the ammonia-water mixture after the expansion in the turbine.

72 **1.1. Comparison studies of KC and ORCs**

73 In the research carried out by Valdimarsson (2003), it was shown that the capital costs of the KC for the exploitation of
74 low temperature heat resources are comparable with those of ORC. Furthermore, it was also demonstrated that, for the
75 same heat input, the power output of the KC resulted higher than that produced by the ORC. Both cycles were analysed
76 with first and second law approach by Rodriguez et al., 2012. From the comparison of the results, it was shown that the
77 KC is capable of producing about 18% more power output than the ORC at comparable costs per energy unit. The
78 research performed by Victor et al. (2013) involved the optimization of ORCs and KC in the 100 – 250°C temperature
79 range with the objective of maximizing the cycles efficiency. They assessed an optimized compositions of a new water
80 – alcohol mixture as working fluid for the KC and demonstrated how this new mixture could increase the efficiency of
81 the cycle, especially in the 220-250° C range. Fu et al. (2013) did a comparison between ORC and KCs in a novel
82 application for the exploitation of geothermal energy waste heat recovery in oil fields. Li and Day (2014) evaluated and
83 compared the performance of KC and trans-critical CO₂ cycles for the exploitation of low temperature enhanced
84 geothermal systems by the means of thermo-economic analysis. The main results were that the KC could achieve a
85 higher thermal efficiency and net power output, while exhibiting lower costs of kWh, mainly due to the lower impact of
86 heat exchanger costs.

87 On the whole, the literature addresses KC as one of the best thermo-economic performing cycles for the exploitation of
88 low temperature geothermal resources. Energy, exergy and exergo-economic analysis to compare dual pressure/dual
89 fluid ORC_s and KC were carried out by Shokati et al. (2015). The turbine was identified as the critical component for
90 both ORCs and KC, holding a high impact both on irreversibilities and investment costs. Among the investigated

91 cycles, the dual-pressure ORCs achieved the highest power output (15% more than the base ORC), whereas KC had the
92 lowest specific energy costs, (66% less than the basic ORC). In his research, Arslan (2010), stated that KC is preferable
93 to the ORCs when the temperature of the heat source is below 413 K.

94 A comparative analysis of KC and ORC thermodynamic performance was carried out by (Bombarda et al., 2009) on a
95 case study involving the recovery of waste heat from two 900 kWe diesel engines. The obtained results demonstrated
96 how the power output of the cycles for medium-high temperature heat sources would be comparable. However, the KC
97 would require a maximum operating pressure considerably higher than the ORC, as well as an increase in power plant
98 complexity. On the other hand, for low temperature heat resources, the KC appears to be competitive. A
99 thermodynamic and thermo-economic comparison of ORCs, KC and TLC (Trilateral Rankine Cycle) for the
100 exploitation of low temperature heat resources, was carried out by Yari et al. (2015). They concluded that the highest
101 power output could be achieved from TLC, while the lowest energy costs from ORC with n-butane as working fluid.

102 At present, very few power plants adopting KC were installed; they confirmed good performance levels. Currently, in
103 Europe there are three only: the geothermal power plant in Husavik, Iceland (Leibowitz and Micak, 1999); and two
104 plants in Germany, built by Siemens between 2007 and 2009 (Knapek and Kittl 2007, Mergner et al., 2013).

105 Several interesting studies on the comparison between KC and ORCs are available, *but a thorough comprehensive*
106 *investigation of the two options with different heat resources, based on the same exergo-economic model, appears to be*
107 *still missing*. Indeed, as it can be noticed from the literature survey, the outcomes are sometimes widely discordant: on
108 one side, there are optimization studies concluding that the best solution is the ORC (Bombarda et al., 2009; Yari et al.,
109 2015). On the other hand, there are studies claiming KC as the best performing power plant over ORCs in the field of
110 binary cycles (Valdimarsson, 2003; Rodriguez et al., 2012; Victor et al., 2013; Fu et al., 2013; Li and Day, 2014;
111 Shokati et al., 2015; Arslan, 2010). The discrepancies found in literature may also depend on the specific characteristics
112 of the resource and on the different applied calculation models for the analysis.

113 In the present study, a thermodynamic and exergo-economic analysis and comparison of the basic ORC, with different
114 working fluids (including mixtures) and cycle conditions (including supercritical cycles), and KCs is presented for two
115 different representative case studies of geothermal resources. Both thermodynamic cycles were designed and optimized
116 from exergy and exergo-economic perspective, in order to achieve the highest possible performance for a fixed heat
117 input.

118 *The main goal of this study* is, therefore, the investigation and comparison of optimized solutions adopting KC and
119 several ORC cycles to the two selected case studies, largely different in size, in order to assess the *optimum suitable*

120 *temperature of the resource and the boundaries of KC – ORC convenience, either from thermodynamic and exergo-*
121 *economic points of view.*

122

123 **2. Methodology**

124 **2.1. Mt. Amiata Case Study**

125 Two real case studies were modelled as the basis to assess the applicability of KC system. The first case study is that of
126 the medium-high enthalpy geothermal field of Mt. Amiata, Italy. It is a water-dominant hydrothermal system localized
127 at 3000-3500 m depth, where the geothermal fluid in the reservoir is at temperature and pressure of about 325° C and
128 250 bar respectively. Currently, this resource is exploited by the single-flash geothermal power plant technology.
129 Indeed, the geothermal fluid, during its ascending path undergoes a flash process at about 600-800 m depth, due to the
130 decrease of the hydrodynamic pressure gradient. The Amiata geothermal field was selected as a case study because of
131 the difficulties encountered in using the local resource with flash power plant technology. The brine is particularly rich
132 in antimony sulphide (Stibnite), which precipitates in the flash drain at temperature below 140°C and is responsible for
133 the scaling of the ducts, causing drastic reductions of the passage sections. In order to prevent the scaling of Stibnite,
134 the introduction of a borehole pump upstream the flash point was proposed, thereby maintaining the geothermal fluid
135 under pressurized liquid conditions, from the extraction to the re-injection reservoir. The required pump head and power
136 were calculated modelling the friction and heat losses in the geothermal fluid extraction duct. This site is also critical
137 because of the pollutants (mainly CO₂, H₂S, Hg and NH₃) contained in the Non-Condensable Gases (NCG, about 7% in
138 volume of the steam fraction). The current technological solution applied to flash power plants is the catalytic gas
139 treatment (patented AMIS process, Baldacci et al., 2005), which guarantees extensive abatement but has relevant costs
140 and affects the power plant availability; moreover, the CO₂ contained in the geothermal resource is released to the
141 atmosphere (Fiaschi et al., 2014).

142 **2.1.1. Borehole pump**

143 One of the topics of this research is closely related to the characteristics of the medium – high temperature geothermal
144 fluid of Mt. Amiata field. It was considered as a pressurized liquid, to be directly reinjected after the heat transfer to the
145 power cycle, in order to reduce the environmental hazard related to the incondensable gas released to the atmosphere
146 such as carbon dioxide, methane and hydrogen sulphide, while avoiding the scaling of silicate and calcium carbonate
147 and inhibit the generation of Stibnite. Another method to avoid the scaling of Stibnite, could be increasing the PH of the
148 fluid. Mechanical or Chemical removal are anyhow necessary when prevention is not suitable: nonetheless, both of

149 them require long periods of downtime (Brown, K., 2011), justifying therefore the investigation of further solutions. In
150 order to fulfil the pressurized liquid condition, the utilization of a borehole pump located inside the well at 800 m depth
151 from the ground level was assumed.

152 The pressurized fluid, after having delivered its sensible heat to the working fluid, is re-injected at a fixed 150°C
153 temperature, in order to avoid any sedimentation of stibnite while ensuring, at the same time, a correct management of
154 the geothermal field.

155 **2.2. Pomarance Case Study**

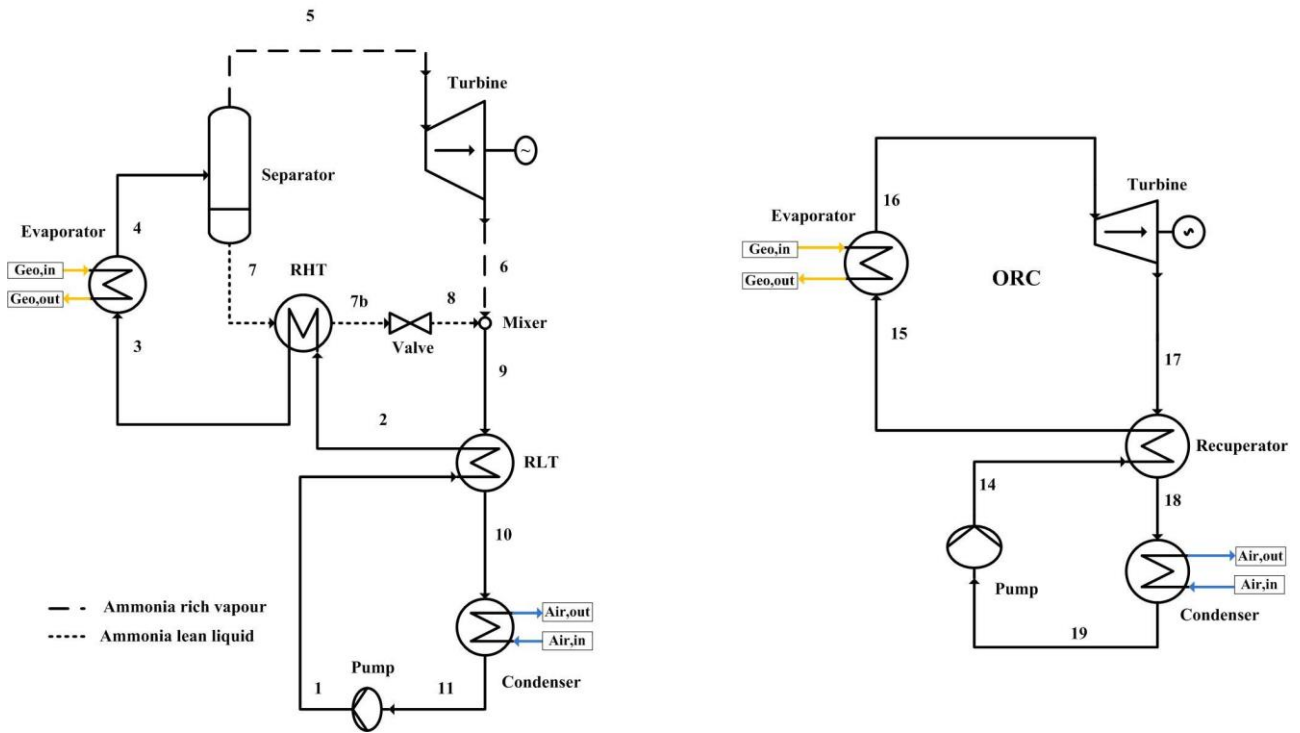
156 In order to verify that KC is preferable to the ORCs for low temperature heat source (Arslan, 2010), a low temperature
157 geothermal resource was also investigated. Specifically, the Pomarance geothermal field was selected as the second
158 case study. Currently, the Pomarance heat resource is exploited for providing heat, through a district-heating network,
159 to the namesake town. The analysed cycles were coupled to the superheated water circuit, which provides heat at 120°
160 C.

161

162 **2.3. Cycles configurations**

163 The main components of the KC are similar to those of an ORC power plant. The main difference is the presence of a
164 separator, which is a specific feature of the KC. The flow splitting allows an improved internal recuperation of the
165 cycle. The schematics of the analysed cycles, KC on the left and ORC on the right, are shown in figure 1. On the
166 working fluid side, the NH₃-H₂O mixture enters the evaporator at point 3 and exits in under-saturated vapour conditions
167 (point 4). The working fluid is not entirely vaporized and it is sent to a vertical separator, which splits the NH₃-H₂O
168 mixture into an ammonia rich vapour (point 5) and an ammonia-lean water-rich saturated liquid (point 7). The
169 ammonia-rich vapour exits from the top of the separator and gets into the turbine, where it expands down to the
170 condenser pressure (point 6). After the expansion, the ammonia-rich vapour is mixed with the ammonia-lean liquid
171 stream, thus producing again the original mixture composition (point 9). Upstream the condenser, two recuperative heat
172 exchangers are included in the process. The Low-Temperature Recovery heat exchanger (RLT) pre-cools the condenser
173 stream and represents the first pre-heating stage, which reduces the final evaporator heat duty. A second, High
174 Temperature heat Recovery process (RHT) takes place between the preheated condenser stream and the ammonia-lean,
175 water-rich mixture. The final result is the reduction of the external heat duties, both for the condenser (points 10-11),
176 and evaporator (points 3-4). A throttle valve (points 7b-8) provides the necessary pressure adjustment before mixing. A
177 pump (points 11- 1) provides the necessary pressure rise from the condenser to the evaporator pressure levels.

178 The analysed ORC basic configuration allows sub-critical, trans-critical and super-critical operations.



179
180 **Figure 1** Schematic of KC (left side) and ORC cycle (right side)

181
182 Figure 2 shows the T-h diagram of the $\text{NH}_3\text{-H}_2\text{O}$ mixture within KC. The continuous black line represents the basic
183 mixture composition. The blue dotted line represents the ammonia – rich vapour expansion and mixing transformations.
184 The yellow dotted line represents the ammonia – lean mixture heat transfer, throttle valve and mixing processes. As it is
185 seen, the recuperated mixture at point 9 still has high temperature and enthalpy, which is favourable for internal heat
186 recuperation.

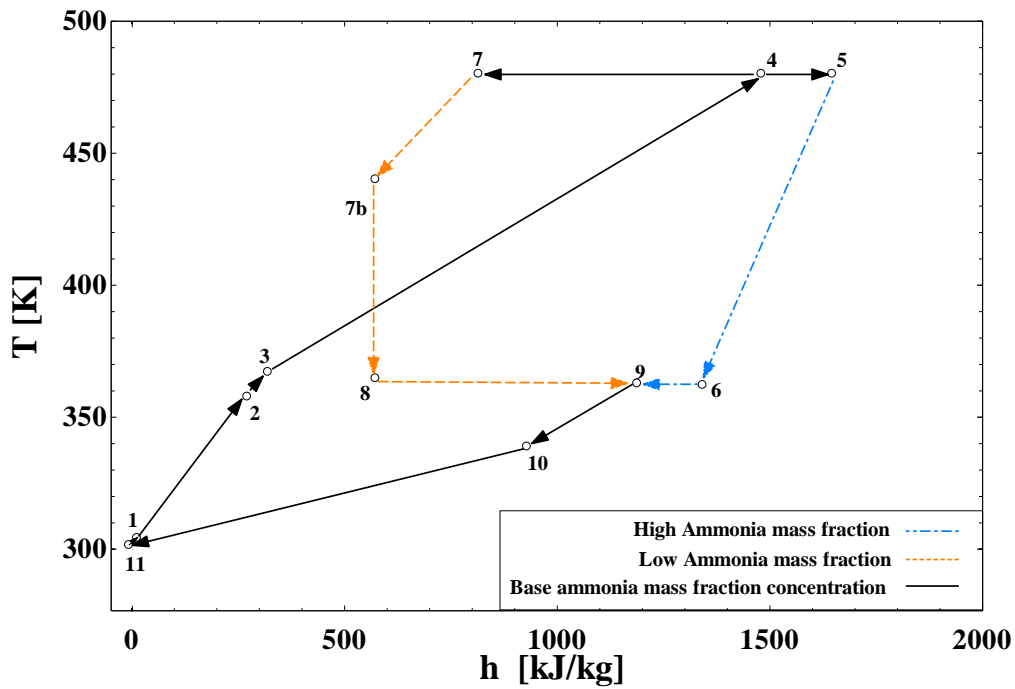


Figure 2T-hdiagram of KC

2.4. Thermodynamic analysis and model validation

The calculation models proposed in this work were developed by Engineering Equation Software (EES, Klein and Nellis, 2012). The main assumptions were the steady operation of power plants and the geothermal fluid modelled as pure water. The implemented equations were numerically solved, with locally-evaluated real fluid cycle properties. When mixtures were considered, the EES-Refprop interface allowed the evaluation of real fluid thermodynamic properties. The fundamental equations (mass and energy balances) were written for each component of the powerplants, following general rules (Klein and Nellis, 2011). The thermodynamic model was validated comparing the results obtained with published literature results (Shokati et al., 2015), as shown in Table 1.

Table 1 KC operating conditions: (a) present work (b) ref. (Shokati et. al., 2015). Input parameters: $T_{geo} = 133,5 \text{ }^{\circ}\text{C}$; $P_{geo} = 3 \text{ bar}$; $x[4] = 0,8455$; $P_{eva} = 40 \text{ bar}$

Stream	Temperature ($^{\circ}\text{C}$)		Ammonia mass fraction		Flow rate (kg/s)	
	a	b	a	b	a	b
1	16.88	15.89	0.8455	0.8455	2.56	2.56
2	31.78	31.3	0.8455	0.8455	2.56	2.56
3	56.85	57.53	0.8455	0.8455	2.56	2.56
4	118.45	118.5	0.8455	0.8455	2.56	2.56
5	118.45	118.5	0.9736	0.9776	1.77	1.75

6	30.37	28.29	0.9736	0.9776	1.77	1.75
7	118.45	118.5	0.5584	0.5679	0.79	0.81
7b	36.55	36.52	0.5584	0.5679	0.79	0.81
8	37.08	37.1	0.5584	0.5679	0.79	0.81
9	36.78	36.52	0.8455	0.8455	2.56	2.56
10	31.96	30.65	0.8455	0.8455	2.56	2.56
11	16.14	15	0.8455	0.8455	2.56	2.56

199

200 2.5 Exergy and Exergo – economic analysis

201 The exergy analysis combines the First and Second Laws of Thermodynamic, allowing the evaluation of the efficiency
 202 of the energy system and the irreversibilities (exergy destructions) of its components (Szargut, J. et al., 1988). The
 203 exergy analysis became one of the most powerful tools for the design and analysis of energy systems and power plants
 204 (Kotas,1985). Indeed, the concept of exergy is able to evaluate the actual thermodynamic values (and thus costs) of
 205 energy flows. Combining economic and thermodynamic analysis, the exergo-economic analysis employs the cost
 206 principles to exergy.

207 The exergo-economic equations of a system, working under steady conditions, are evaluated from the balance of the
 208 input and output costs:

$$209 \sum_{\text{output}} \dot{C}_{P,\text{tot}} = \sum_{\text{input}} \dot{C}_{F,\text{tot}} + \dot{Z}_{\text{tot}}^{\text{CI}} + \dot{Z}_{\text{tot}}^{\text{OM}} \quad (1)$$

210 Where:

- 211 • $\dot{C}_{P,\text{tot}}$ is the output product cost [€/s]
- 212 • $\dot{C}_{F,\text{tot}}$ is the fuel cost (or any another required resource necessary to the operation of the component) [€/s]
- 213 • $\dot{Z}_{\text{tot}}^{\text{CI}}$ is the specific capital cost [€/s]
- 214 • $\dot{Z}_{\text{tot}}^{\text{OM}}$ is the specific operation and maintenance cost [€/s]

215 $\dot{Z}_{\text{tot}}^{\text{CI}}$ e $\dot{Z}_{\text{tot}}^{\text{OM}}$ arecalculated dividing the total annual investments, operation and maintenance costs (coming from the
 216 economic analysis), by the total yearly working time, expressed in suitable units. Their sum is the overall cost rate \dot{Z} :

$$217 \dot{Z} = \dot{Z}_{\text{tot}}^{\text{CI}} + \dot{Z}_{\text{tot}}^{\text{OM}} \quad (2)$$

218 Table 2 summarizes the exergo-economic balances and the auxiliary equations (Bejan, A., et al., 1996), which are logic
 219 statements that allow defining the missing number of conditions to solve the cost equations applied to each component.

220 **Table 2** –Exergo-economic balance equations of power plant components

	KC	ORC Cycle
Evaporator	$c_4 \cdot \dot{E}X_4 = c_3 \cdot \dot{E}X_3 + \dot{C}_{fuel} + \dot{Z}_4$ $\dot{C}_{fuel} = c_{fuel,kj} \cdot (\dot{E}X_{GEO_{in}} - \dot{E}X_{GEO_{out}})$	$c_{16} \cdot \dot{E}X_{16} = c_{15} \cdot \dot{E}X_{15} + \dot{C}_{fuel} + \dot{Z}_{14}$ $\dot{C}_{fuel} = c_{fuel,kj} \cdot (\dot{E}X_{GEO_{in}} - \dot{E}X_{GEO_{out}})$
Separator	$c_5 \cdot \dot{E}X_5 + c_7 \cdot \dot{E}X_7 = c_4 \cdot \dot{E}X_4 + \dot{Z}_5$ $\frac{c_5 \cdot \dot{E}X_5 - c_4 \cdot \dot{E}X_4}{\dot{E}X_5 - \dot{E}X_4} = \frac{c_7 \cdot \dot{E}X_7 - c_4 \cdot \dot{E}X_4}{\dot{E}X_7 - \dot{E}X_4}$	-
Turbine	$c_{W_{tkj}} \cdot \dot{W}_T + c_6 \cdot \dot{E}X_6 = c_5 \cdot \dot{E}X_5 + \dot{Z}_6$ $c_6 = c_5$	$c_{W_{tkj}} \cdot \dot{W}_T + c_{17} \cdot \dot{E}X_{17} = c_{16} \cdot \dot{E}X_{16} + \dot{Z}_{15}$ $c_{16} = c_{17}$
Mixer	$c_9 \cdot \dot{E}X_9 = c_6 \cdot \dot{E}X_6 + c_8 \cdot \dot{E}X_8 + \dot{Z}_7$	-
Throttle valve	$c_8 \cdot \dot{E}X_8 = c_{7b} \cdot \dot{E}X_{7b} + \dot{Z}_8$	-
High Temperature Recuperator	$c_{7b} \cdot \dot{E}X_{7b} + c_3 \cdot \dot{E}X_3 = c_7 \cdot \dot{E}X_7 + c_2 \cdot \dot{E}X_2 + \dot{Z}_3$ $c_7 = c_{7b}$	$c_{18} \cdot \dot{E}X_{18} + c_{15} \cdot \dot{E}X_{15} = c_{17} \cdot \dot{E}X_{17} + c_{14} \cdot \dot{E}X_{14} + \dot{Z}_{16}$ $c_{17} = c_{18}$
Low Temperature Recuperator	$c_{10} \cdot \dot{E}X_{10} + c_2 \cdot \dot{E}X_2 = c_9 \cdot \dot{E}X_9 + c_1 \cdot \dot{E}X_1 + \dot{Z}_2$ $c_9 = c_{10}$	-
Condenser	$c_{11} \cdot \dot{E}X_{11} = c_{10} \cdot \dot{E}X_{10} + \dot{Z}_1$	$c_{19} \cdot \dot{E}X_{19} = c_{18} \cdot \dot{E}X_{18} + \dot{Z}_{17}$
Pump	$c_1 \cdot \dot{E}X_1 = c_{11} \cdot \dot{E}X_{11} + c_{W_{pkj}} \cdot \dot{W}_{pump} + \dot{Z}_9$ $c_{W_{pkj}} = c_{W_{tkj}}$	$c_{14} \cdot \dot{E}X_{14} = c_{19} \cdot \dot{E}X_{19} + c_{W_{pkj}} \cdot \dot{W}_{pump} + \dot{Z}_{18}$ $c_{W_{pkj}} = c_{W_{tkj}}$

221

222 2.6 Investment and O&M costs

223 In order to determine the investment and O&M costs ($\dot{Z}_{tot}^{CI} + \dot{Z}_{tot}^{OM}$) of the two proposed power plants, an economic
 224 analysis was carried out. The first step was the calculation of the components costs, which was done following the

225 methodology proposed in (Turton, et al., 2003). The components costs were determined from a standard mathematical
226 relationship, which was subsequently improved with correction factors accounting for component class, working
227 pressure and equipment materials. Finally, the obtained value was actualized to the reference year (2015) through the
228 CEPCI (Chemical Engineering Plant Cost Index) inflation index (Chemical Engineering, 2015).

229 The Operation and Maintenance costs (O&M) of each component were determined as a fraction (1.5%) of the Purchased
230 equipment costs (PEC), as suggested by Schuster (Schuster, A., et al. 2009).

231 The calculation of the Total Capital Investment cost (TCI) is presented in detail in Appendix A. Once the TCI was
232 calculated, knowing the total yearly working hours of the power plant, it was possible to determine \dot{Z} in €/s. In this case,
233 we assumed 7446 [h/year] working time, which is a realistic value for geothermal power plants (Shokati, et. al., 2015).

234 The final outcome of the exergo-economic analysis is the cost of the produced kWh (c€/kWh).

235

236 **3. Results**

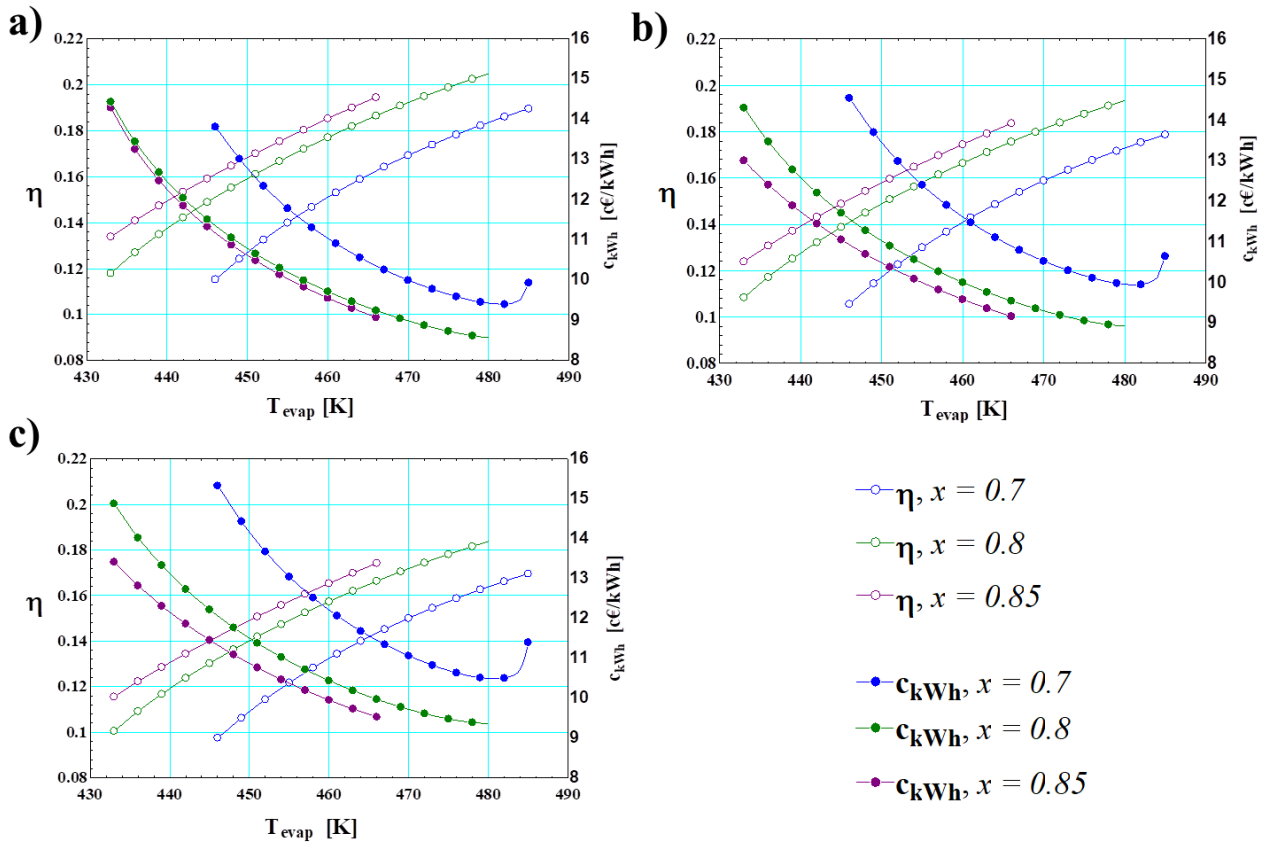
237 **3.1. Power Cycles Optimization**

238 The main parameters affecting the performance of the KC are the maximum and minimum temperature and pressure at
239 evaporator and condenser output and the ammonia mass fraction in the rich solution at the separator inlet. Therefore, a
240 sensitivity analysis to these fundamental parameters was done, in order to maximise the thermal efficiency of the power
241 plant and minimize the unit cost of the produced energy, for both high and low temperature case studies. For each
242 reference case, a comparison with optimised ORC solutions was also carried out.

243 In the Mt. Amiata case study, figure 3 (a, b and c) displays the KC efficiency and produced energy unit cost vs.
244 maximum cycle temperature (i.e. at evaporator exit) for three different ammonia mass fractions and condenser
245 pressures. Due to the fixed upper temperature level, the cycle is improved at lower condenser pressure, thus the
246 efficiency is higher and the energy unit costs are reduced.

247 With 0.8 ammonia mass fraction (base solution upstream the separator), the highest values of thermal efficiency are
248 achieved. By the way, lower ammonia concentrations allow the exploitation of higher maximum temperature levels. On
249 the other hand, higher ammonia concentrations give better performance with lower temperature heat sources. For these
250 reasons, even the lowest unit energy cost is found at 80% ammonia mass fraction.

251

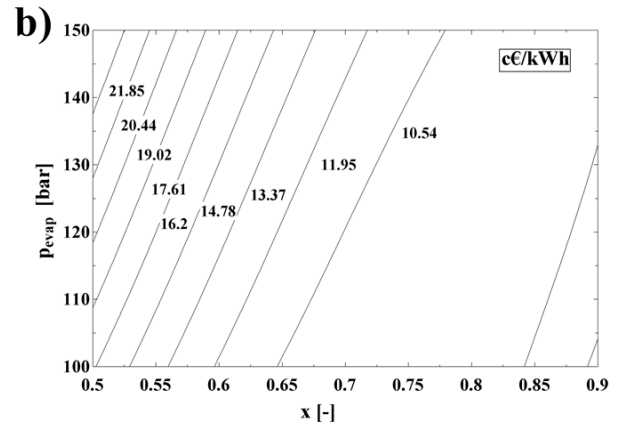
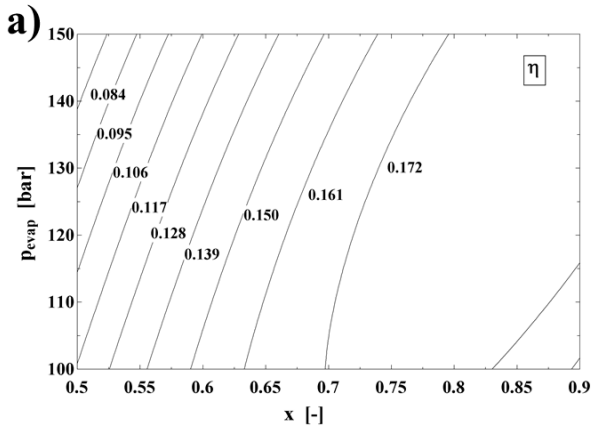


252

253 **Figure 3** Thermal efficiency and produced power unit cost for KC Cycle, as a function of Evaporator temperature, ammonia mass fraction and
 254 condenser pressure. Evaporator pressure = 114 bar; Condenser pressure = 7 bar (a); 9 bar (b); 11 bar (c)

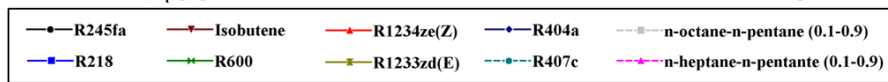
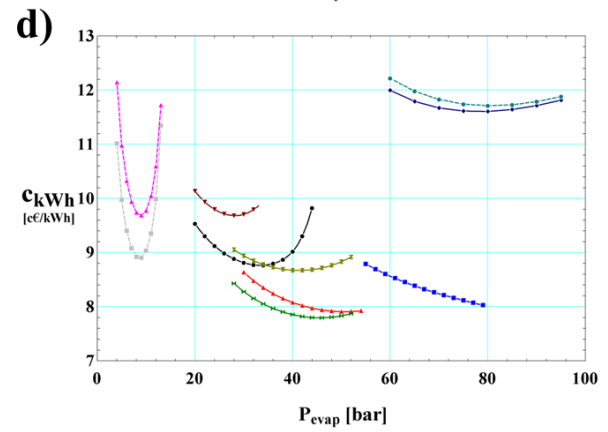
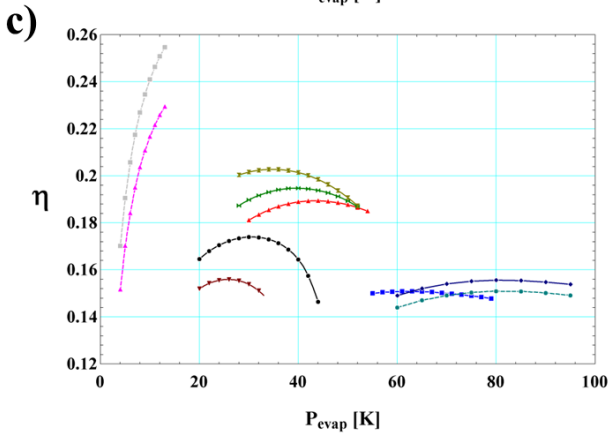
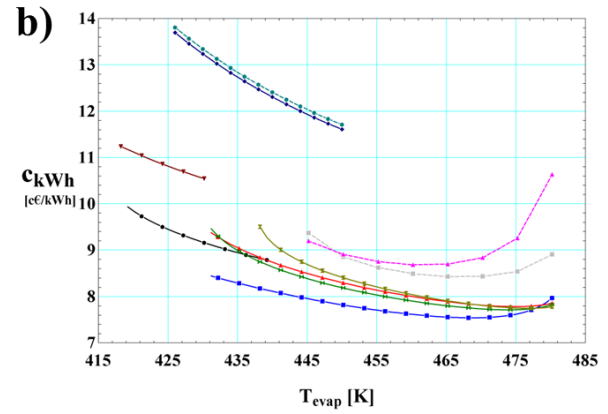
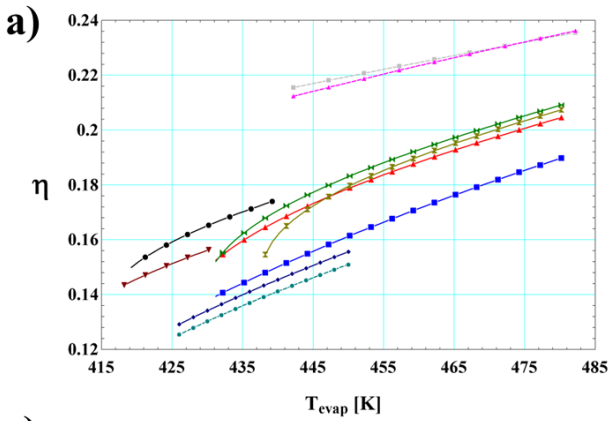
255

256 Figure 4 shows the contours of the KC efficiency (a) and produced energy unit costs (b) vs. evaporator pressure, at
 257 variable ammonia mass fraction. Higher values imply higher evaporator pressures, in order to achieve high efficiencies
 258 and low unit energy costs. The parametric analysis allowed, therefore, the determination of the optimal evaporator
 259 pressure to maximize the cycle efficiency and minimize the unit costs of produced energy.



260

261 **Figure 4** Contours of Thermal efficiency (a) and produced energy unit cost (b, [c€/kWh]) for KC, vs. evaporator pressure and ammonia mass fraction.
 262 Evaporator Temperature = 480 K; Condenser pressure = 9 bar

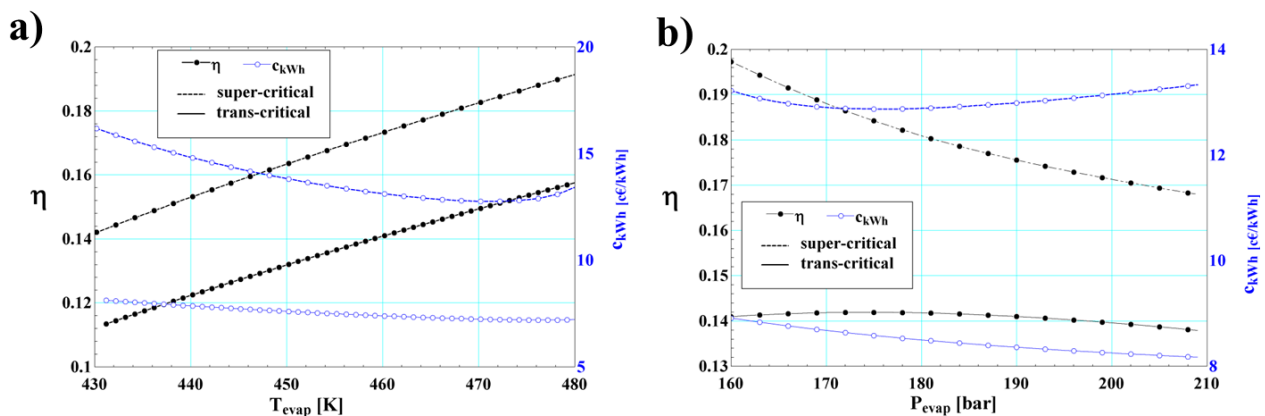


263

264 **Figure 5** ORC efficiency and produced energy unit cost as a function of Evaporator temperature (a-b) and pressure (c-d)

265 The same parametric analysis was carried out for the ORC. Figures 5 shows the efficiency and produced energy unit
 266 cost of the ORC, as a function of evaporator pressure (a) and temperature (b) for several different working fluids, from
 267 pure substances like R245fa or R600, to mixtures such as R404a or n-heptane/n-pentane (0.1-0.9). Specifically, the

268 selection and composition of the hydrocarbon mixtures proposed by Oyewumni, O.A., et al., 2017 was also considered
 269 here. Furthermore, the present work also includes the performance and cost analysis of CO₂ cycle, under both trans and
 270 super critical conditions. Figure 6 shows how the latter achieves higher efficiency, but has the disadvantage of a higher
 271 produced energy unit cost. Due to the fixed upper temperature level (which was selected as the maximum achievable
 272 temperature of the fluid), the cycle efficiency shows an optimizing pressure trend, which is strongly dependent on the
 273 fluid type. On the other hand, as it was expected, higher efficiency values and lower produced energy unit costs were
 274 obtained at higher maximum cycle temperature.



275
 276 **Figure 6** Efficiency and produced energy unit cost for the ORC Cycle, as a function of the maximum temperature (a) and the higher pressure level (b)
 277 of the cycle. ORC Working Fluid = Carbon Dioxide

279 3.2. Exergy analysis: results

280 3.2.1. Mt. Amiata case study

281 The performance data of the considered power cycles for the high temperature case (Mt. Amiata) are summarized in
 282 table 4. In this site, the geothermal fluid is available at 212°C and it is re-injected at 150°C. The best matching
 283 thermodynamic cycle to the geothermal fluid resource is the one with super-critical CO₂, which, however, still has a
 284 worse matching than KC for a large field. With R1233zd(E) and the hydrocarbon mixtures (n-octane/n-pentane 0.1/0.9
 285 mass fraction and n-heptane/n-pentane 0.1/0.9 mass fraction) as working fluids, the first law efficiency achieved values
 286 higher than 20%, which are reduced to about 18 % when including the power consumed by the borehole pump.

287 Considering the same amount of available geothermal heat input for all the thermodynamic cycles, the KC solution
 288 gives better efficiency than the ORCs working with R245fa, R218, trans critical and super critical CO₂, R404a, R407c
 289 and R1234ze(Z). On the other hand, the KC efficiency is lower compared to ORCs working with Isobutene, R600,
 290 R1233zd(E) and the investigated hydrocarbon mixtures, as shown in table 4.

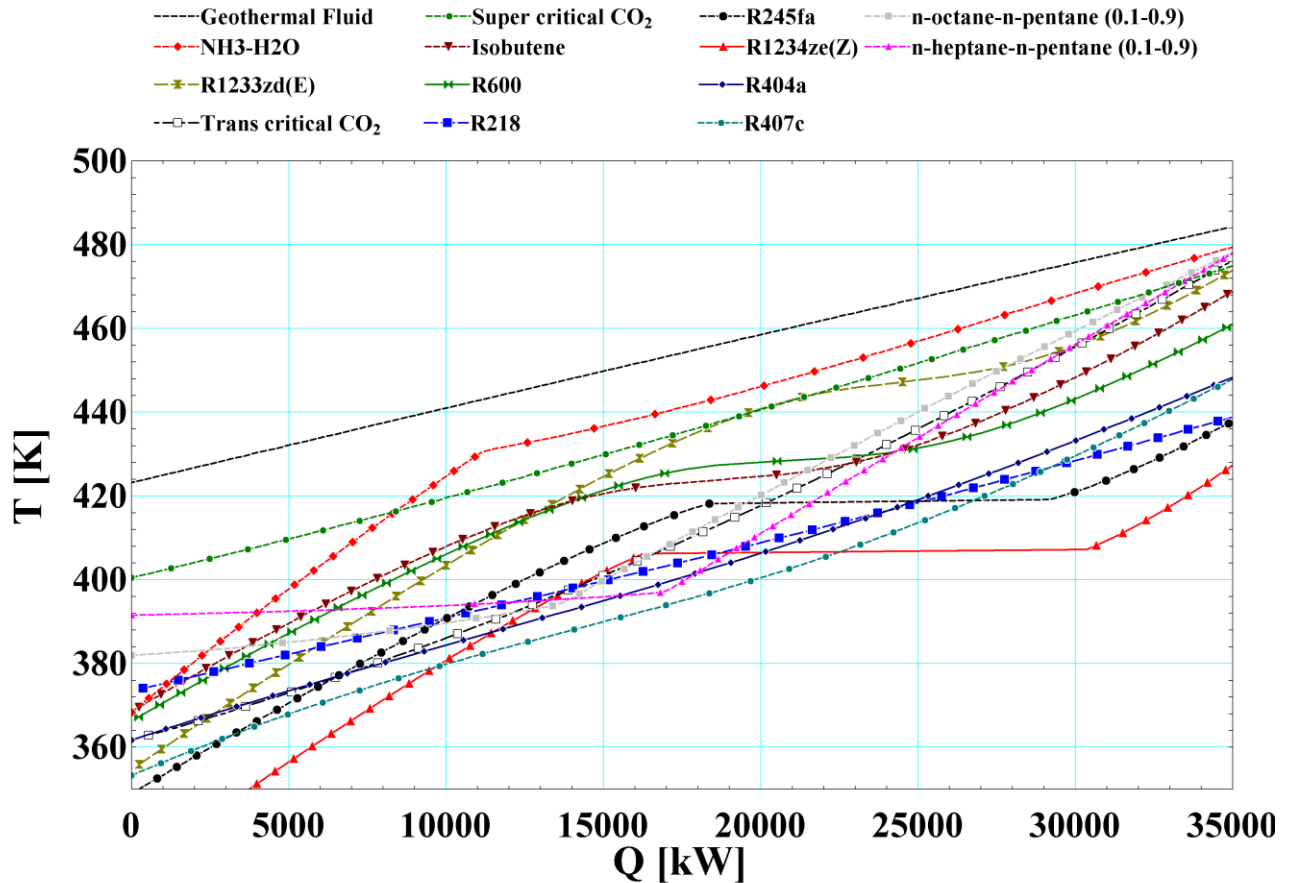
291 Isobutene, R600, R404a, R407c and R1233zd(E) have a trans-critical behaviour, due to the fixed temperature and
292 pressures in the case study. These kinds of cycles allow a better matching of the curves at the evaporator, as shown in
293 figure 7, where the behaviour of the cycle higher temperature side, allowing the highest thermal efficiency at fixed
294 upper and lower temperature bounds of the heat sources (i.e. geothermal and environment), are considered. The good
295 matching of geothermal and working fluid heat capacities grants limited irreversibility in heat transfer, thus allowing a
296 better exploitation of the geothermal resource. Also the KC, due to the zeotropic NH₃-H₂O working fluid mixture and
297 the hydrocarbon mixtures, which allow a non – isothermal vaporization behaviour, hold a good matching level with the
298 geothermal fluid behaviour at the evaporator. It makes KC and ORC with hydrocarbon mixtures attractive compared to
299 ORCs with pure fluids and isothermal vaporization behaviour.

300 R218, R404a, R407c and trans critical CO₂ cycles exhibit the worst cycle performance, because their thermodynamic
301 efficiencies are heavily affected by the relatively high power demand of the recirculation pump: it requires 26.2% and
302 39% respectively of the total cycle power output. On the contrary, for all the other fluids (except super critical CO₂,
303 which nonetheless achieves higher cycle efficiency), the recirculation pump power has a lower relative influence,
304 variable between 6.5% and 8.9% of the overall turbine power output. R1233zd(E) presents one of the highest power
305 plant performance and the lowest produced energy unit costs. Besides, this working fluid is a new generation organic
306 fluid (HFO, derived from the common used R134a), having zero Ozone Depletion Potential (ODP) and very low Global
307 Warming Potential (GWP) of 5. These favourable features suggest the R1233zd(E) selection for the high temperature
308 case of Mt. Amiata.

309

310 **Table 4** Performance comparison between KC and ORC cycles for the High Temperature case (Mt. Amiata)

Performance Parameter			KC	ORC											
				R245fa	Isobutene	R600	R218	Trans-critical Carbon Dioxide	Super-critical Carbon Dioxide	R1234ze(Z)	R1233zd(E)	R404a	r407c	n-octane n-pentane (0.1-0.9)	n-octane n-pentane (0.1-0.9)
Heat Exchanged	Evaporator	[kW]	35528	35528	35528	35528	35528	35528	35528	35528	35528	35528	35528	35528	
	HT Recuperator	[kW]	1485	-	-	-	-	-	-	-	-	-	-	-	
	LT Recuperator	[kW]	7936	1114	11052	10763	27077	13132	68975	2121	7260	15335	10127	39502	28545
	Condenser	[kW]	28648	29347	28533	28609	30169	30486	28847	30007	28394	30000	30166	28221	28292
Power	Turbine	[kW]	7458	6608	7682	7564	7257	8910	10309	5913	7723	7216	6609	7417	7368
	Recirculation pump/compressor	[kW]	578.1	427.1	686.1	645	1898	3472	3627	392.5	588.5	1688	1247	109.3	131.1
	Borehole pump	[kW]	897.5	897.5	897.5	897.5	897.5	897.5	897.5	897.5	897.5	897.5	897.5	897.5	897.5
First Law Efficiency	[-]	0.1937	0.174	0.1969	0.1948	0.1509	0.1545	0.1881	0.1554	0.2008	0.1556	0.1509	0.2057	0.2037	
Global Power Plant Efficiency	[-]	0.1684	0.1487	0.1716	0.1695	0.1256	0.1293	0.1628	0.1301	0.1755	0.1303	0.1257	0.1804	0.1784	

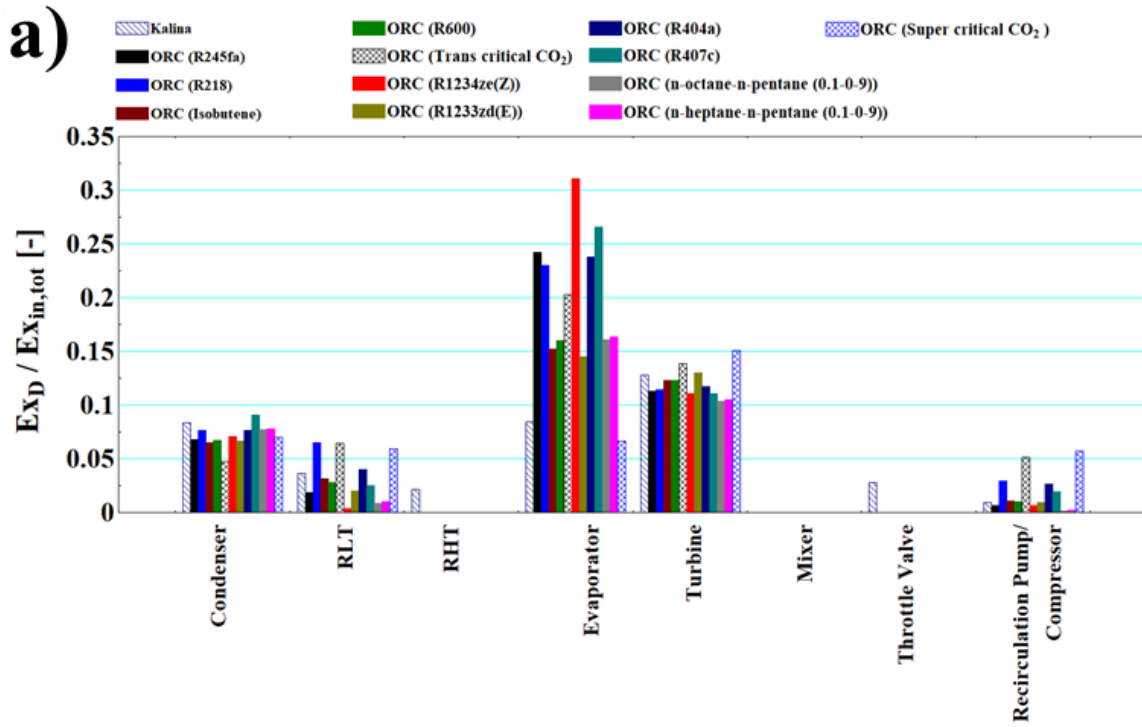


311

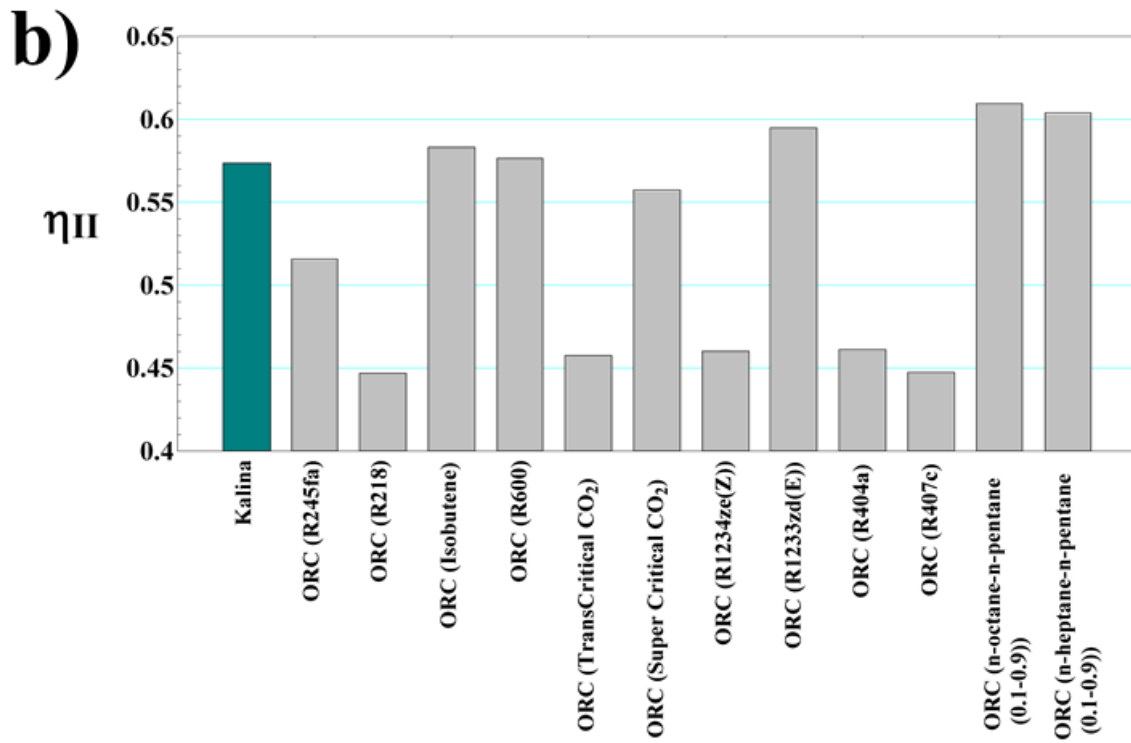
312 **Figure 7** Comparison of heat transfer temperature profiles inside the evaporator, for the Mt. Amiata case study. The dashed black line represents the
 313 cooling curve of the geothermal fluid.

314 Figure 8 shows the non-dimensional exergy destruction of the components in the power cycles. The exergy input was
 315 fixed at the same value for each thermodynamic cycle. As evident from figure 8, the highest exergy destruction source
 316 both for KC and ORC cycles is the evaporator. Generally, trans-critical and super critical working fluids and -zeotropic
 317 mixtures show a good matching with the heat transfer line of the geothermal fluid resource, thus generating relatively
 318 moderate heat transfer exergy destruction. The second highest irreversibility source is the turbine. The only case where
 319 the highest exergy destruction is in the turbine and not in the evaporator is for the super critical CO₂ cycle. This is
 320 mainly due to the very good matching of the evaporator curves and the high power output of the turbine.

321 Depending on the thermodynamic cycle, the device allowing the increase of cycle pressure (namely the recirculation
 322 pump or the compressor), strongly affects the overall exergy destruction. Indeed, as evident from figure 8, R218,
 323 R404a, R407c and trans critical and super critical CO₂ cycles hold far higher exergy destruction than the other working
 324 fluids. This is mainly due to the working fluids condition, which is transcritical (or supercritical in one case of CO₂),
 325 therefore requiring higher compression power input.



326



327

328

Figure 8a) Component exergy destruction comparison between KC and ORCs; b) Second law efficiency comparison between KC and ORCs

329

330

331 **3.2.2.Low temperature case study: Pomarance geothermal site**

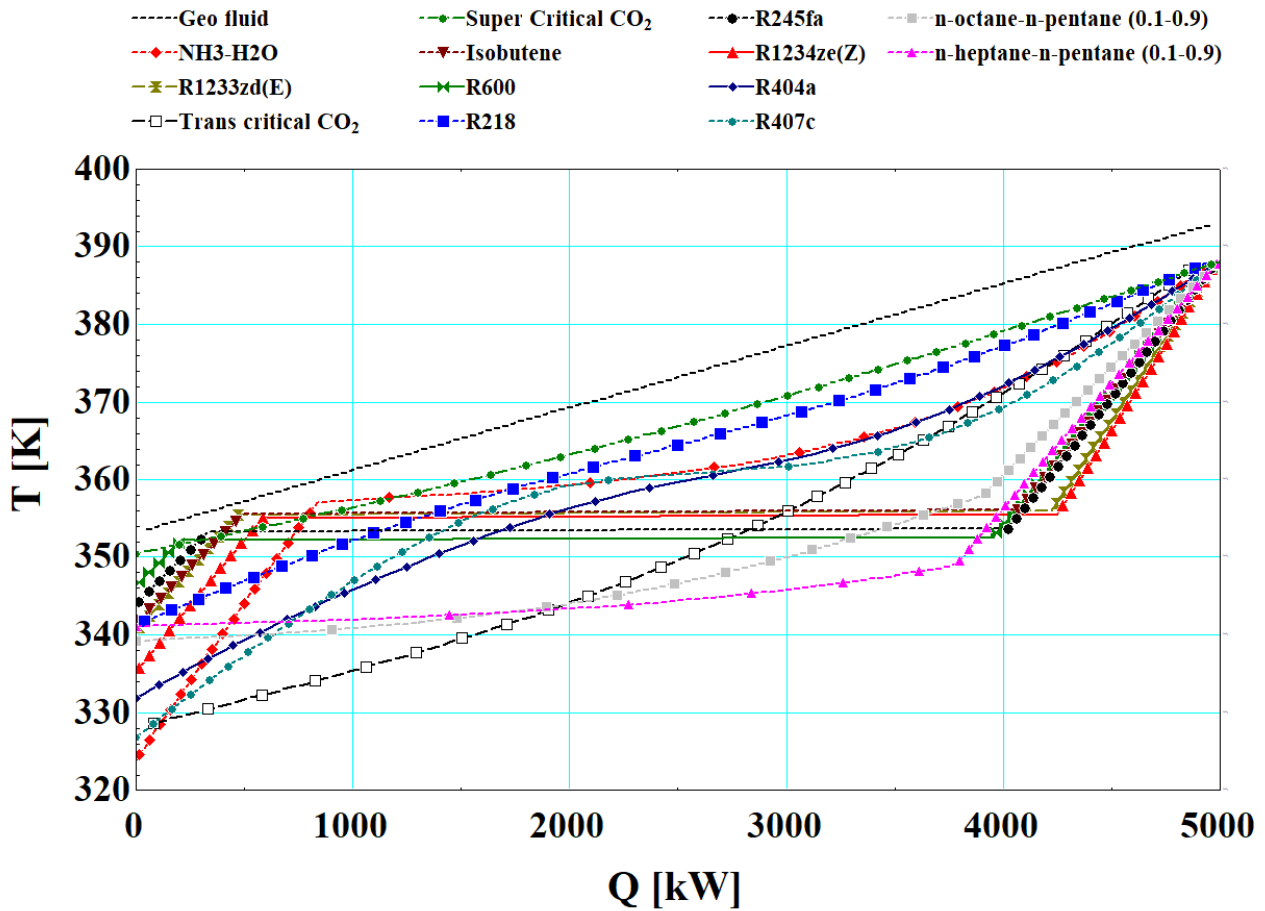
332 The performance data of the investigated cycles for the low temperature case study of Pomarance geothermal site are
333 summarized in table 5.

334 In this site, where the resource is at the low 120°C temperature level and is released at 80°C, the best heat transfer
335 matching between thermodynamic cycle and the geothermal fluid curve is the ORC working with super critical CO₂,
336 nearly followed by the ORC with R218 and the KC. Nevertheless, the super critical CO₂ cycle does not hold the highest
337 performance. This is mainly attributable to the high power required for the compression of the fluid upstream the high
338 temperature heat exchanger. It reduces the efficiency of the power cycle, thus hindering the interesting thermal
339 behaviour potential of this fluid, which, consequently, exhibited performance at the same level of the other working
340 fluids.

341 As for the Mt. Amiata case study, R218, R404a, R407c and CO₂ cycle were trans-critical, differently from all the other
342 ORC working fluids. The vaporization of the other ORC fluids was at constant temperature, thus not allowing a good
343 matching of the evaporator curves to the geothermal fluid behaviour, as shown in figure 9. Nevertheless, the better cycle
344 efficiency of the other fluids, generally more suitable to low temperatures, counterbalanced the higher matching
345 features of the trans-critical R218 and the super and trans critical CO₂. On the whole, the poor matching of the evaporator
346 curves with subcritical cycles brought to moderate values of the first and second law efficiencies, thus the KC showed
347 its far better potential (table 5 and figure 10). Due to the better matching of the heat transfer composite curves at the
348 evaporator, the efficiency of the KC was found at 23 to 42% higher than that of the ORCs, for all the considered fluids
349 including CO₂ cycles.

350 **Table 5** Performance comparison between KC and ORC cycles for the Low Temperature case (Pomarançe)

Performance parameter	KC	ORC												
		R245fa	Isobutene	R600	R218	Trans-critical Carbon Dioxide	Super-critical Carbon Dioxide	R1234ze(Z)	R1233zd(E)	R404a	r407c	n-octane n-pentane (0.1-0.9)	n-octane n-pentane (0.1-0.9)	
Heat Exchanged	Evaporator [kW]	5000	5000	5000	5000	5000	5000	5000	5000	5000	5000	5000	5000	5000
	HT Recuperator [kW]	313.4	-	-	-	-	-	-	-	-	-	-	-	-
	LT Recuperator [kW]	347.1	1044	927.4	1114	2015	909	9647	609	842	923.5	504.5	3731	2547
	Condenser [kW]	4356	4521	4503	4529	4518	4627	4495	4517	4510	4541	4549	4567	4582
Power	Turbine [kW]	674.3	492.3	520.8	488.8	636.4	712.1	900.2	497.5	502.7	589.6	546.3	437.4	423
	Recirculation Pump/compressor [kW]	29.68	12.97	23.58	18	153.8	339.2	394.6	14.62	11.95	130.3	95.21	4.35	4.37
First Law Efficiency	[-]	0.1289	0.0958	0.0994	0.0941	0.0965	0.0746	0.1011	0.0966	0.0982	0.0919	0.0902	0.0866	0.0837

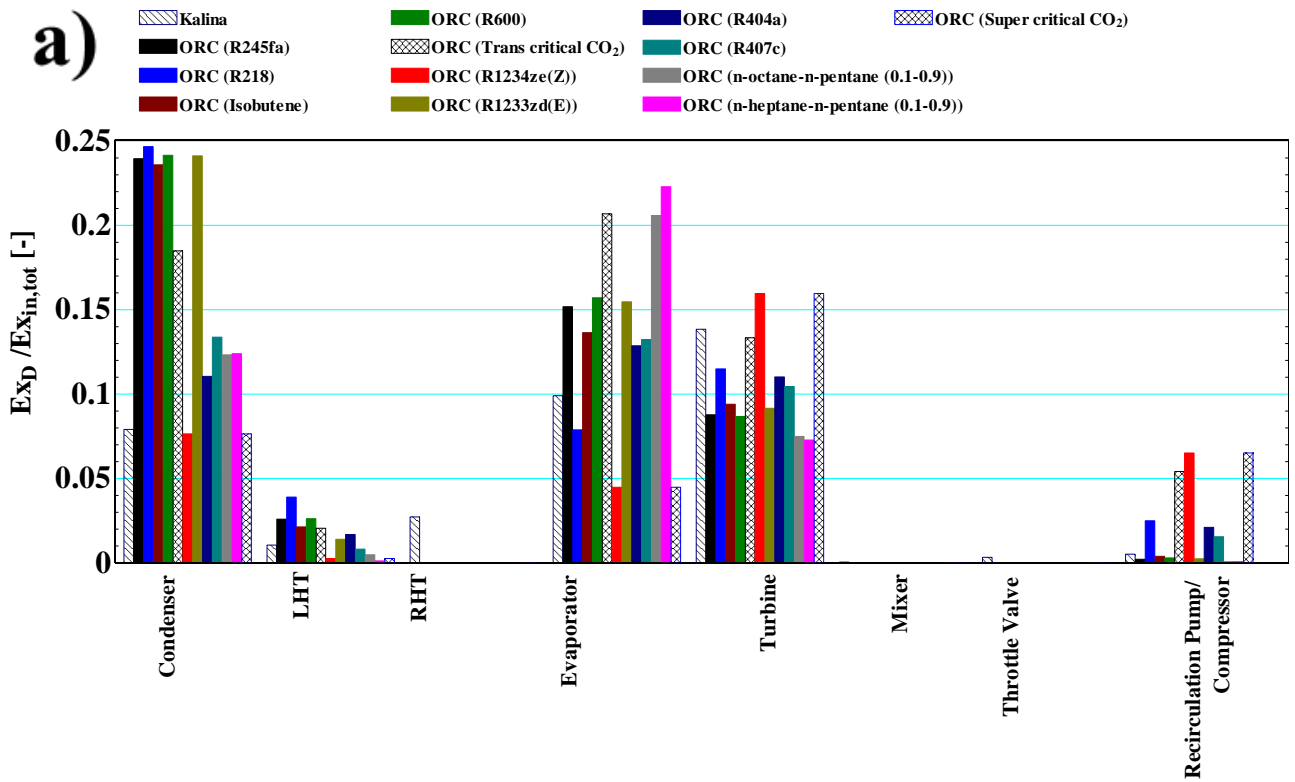


351

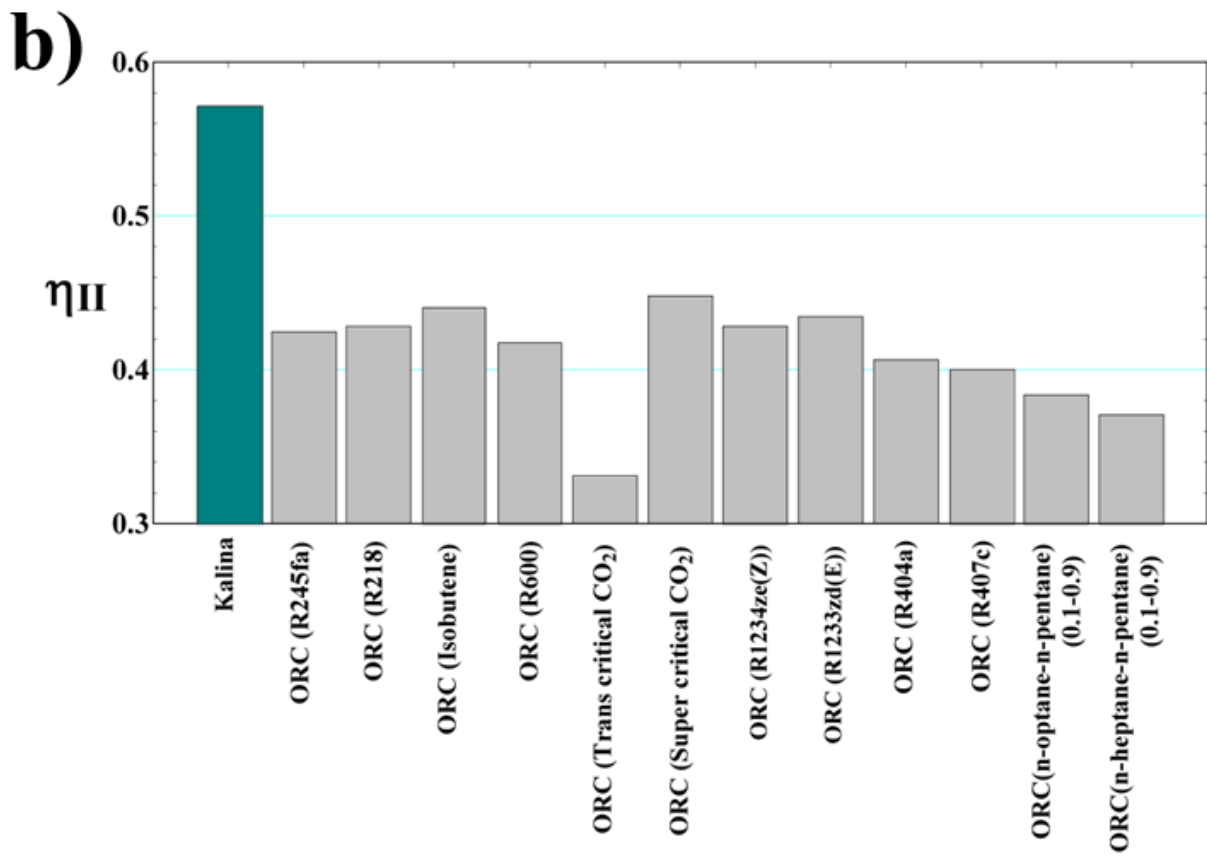
352 **Figure 9** Thermal profiles comparison inside the evaporator, for the Pomarance case study. The dashed black line represents the cooling curve of the
 353 geothermal fluid

354 The main advantage of using a zeotropic mixture as working fluid is its variable phase change temperature, which
 355 allows low values of exergy destruction at the evaporator and, even more, at the condenser. It is clearly shown in figure
 356 10a. In this case, this effect is dominant and, for this reason, the KC showed the best performance. The variable
 357 temperature phase change, both in vaporization and condensation, allows the achievement of a second law efficiency
 358 about 10 points higher than for the other ORCs (figure 10b). Compared to the ORCs, the overall exergy destruction of
 359 the KC case was reduced from 23 to 35%, as a result of the lower exergy destruction of the cycle components, with the
 360 only exception of the turbine, due to the higher enthalpy of the output flow. However, it is partially recovered in the low
 361 temperature recuperator (RLT, figure 1).

362



363



364

365 **Figure 10a)** Comparison of components relative exergy destructions between KC and ORCs; b) Second law efficiency comparison between KC and
 366 ORCs

367

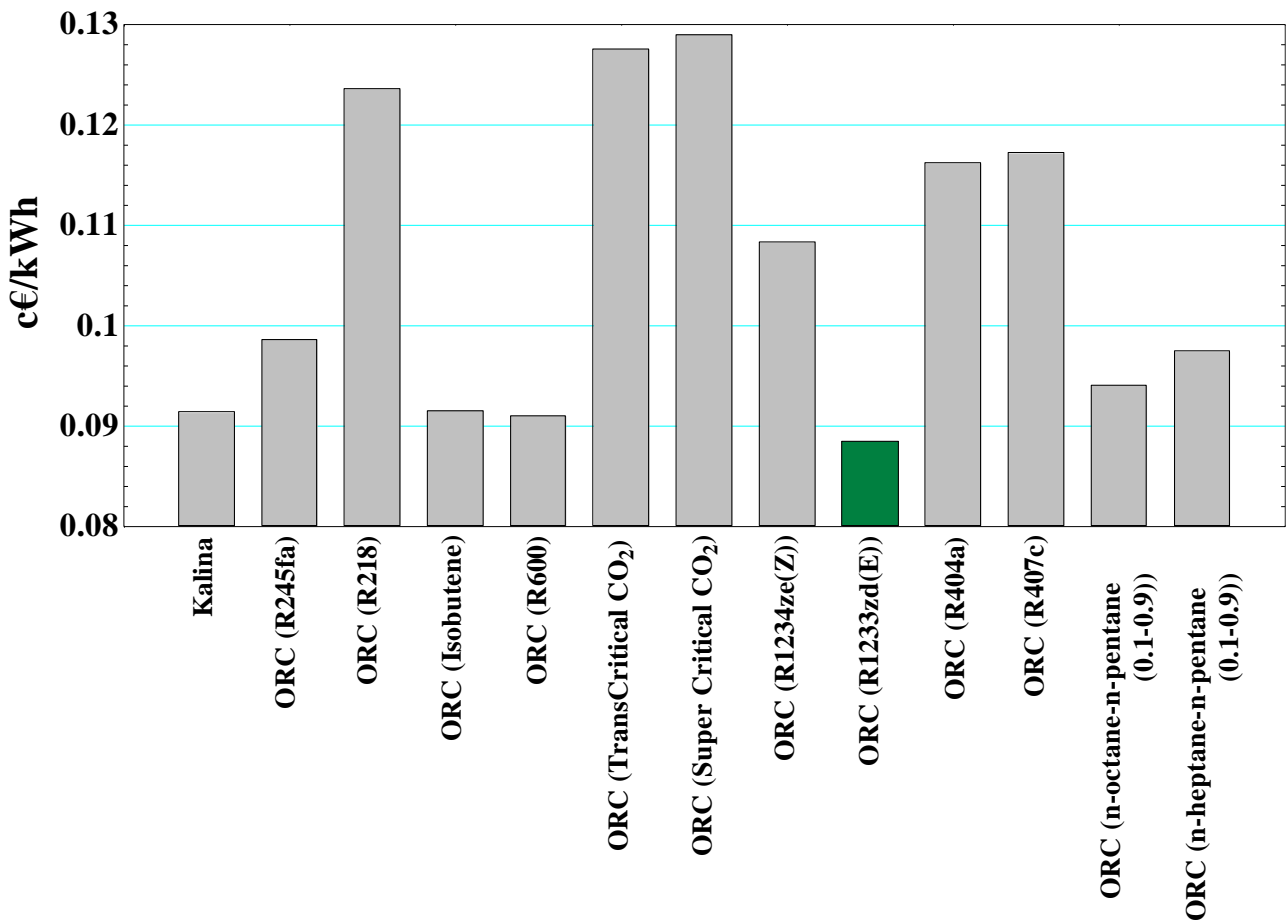
368 **3.3. Exergo-economic analysis: results**

369 **3.3.1.Mt. Amiata case study**

370 The exergo-economic analysis allows the assessment of the cost of electricity generation of the proposed power cycles
371 for the two different representative case studies in the Italian context. Currently, the average national electricity
372 production cost in Italy from geothermal powerplants is about 9.5 c€/kWh in the range of 5 MW size and about 7.5
373 c€/kWh in the 20 MW size (AEEG, 2013).

374 In the here presented high temperature case study, the lowest electricity cost (8.85 c€/kWh) was achieved with the ORC
375 with R1233zd(E) as working fluid. On the contrary, the highest electricity cost (12.90 c€/kWh) was calculated with the
376 CO₂super critical cycle. Due to the well-matching of the heat transfer curves at the evaporator, the KC exhibited a
377 moderate electricity cost (9.12 c€/kWh), in spite of the more complex power plant layout. Figure 11 summarizes the
378 calculated electricity cost for all the analysed power cycles and working fluids: the KC showed values at the same level
379 of the ORCs with the highest performing fluids.

380



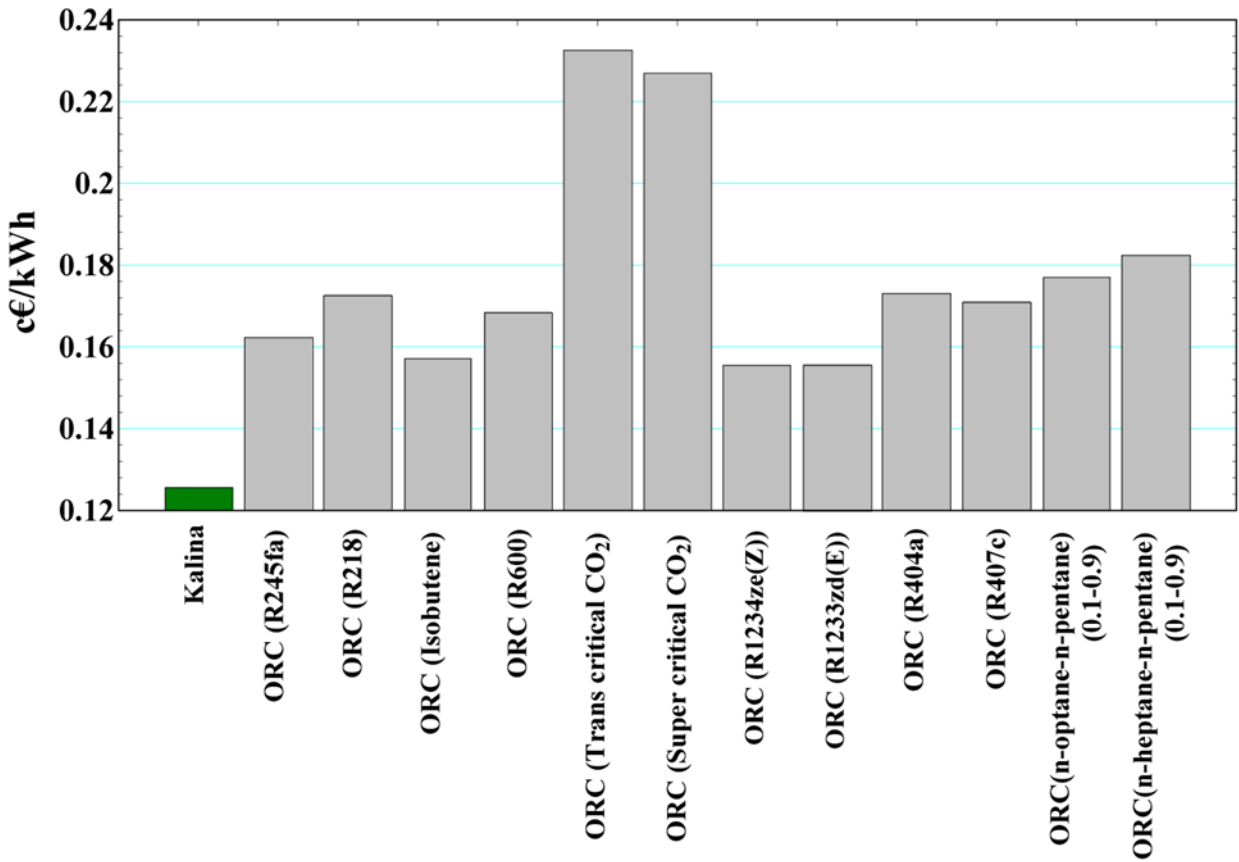
381

382 **Figure 11** Comparison of electricity costs for the analysed power plants, Mt. Amiata case study.

383

384 3.3.2. Low temperature case study: Pomarance geothermal site

385 Figure 12 shows the results of the exergo-economic analysis for the Pomarance case study. The lowest electricity cost
386 was achieved by the KC at 12.53 c€/kWh. On the contrary, the trans critical CO₂ cycle showed the highest electricity
387 production costs (about 23 c€/kWh). On the whole, the total investment cost of KC resulted higher than R245fa,
388 Isobutene, R600, R404a, R407c, R1234ze(Z) and R1233zd(E), n-octane/n-pentane and n-heptane/n-pentane ORCs by
389 8.96%, 9.65%, 4.22%, 3.96%, 10.65, 17.45%, 13%, 12.83% and 13.36%, respectively. Despite the higher capital
390 investment cost, the higher power production due to the better cycle efficiency and the improved heat transfer matching
391 at the boiler with the available geothermal resource (which brought to higher 2nd Law efficiency of the whole system)
392 allowed the reduction of the electricity cost between 24% and 34% compared to the ORCs. This basically agrees with
393 literature (Shokati, et. al., 2015), which addresses KC as one of the most economically viable solutions when dealing
394 with low temperature resources, like Pomarance case study.



395

396 **Figure 12** Comparison of electricity costs for the analysed power plants, Pomarance case study

397

398 **4. Case studies results: comparison and conclusions**

399 The main goal of this study was the comparison of KC and ORC binary cycles to exploit two different representative
 400 geothermal resources by the means of an exergo-economic approach.

401 The main results are summarized in table 6. Specifically, for the high-temperature resource case study (Mt. Amiata), the
 402 ORC with n-octane/n-pentane mixture (0.1-0.9 mass fraction) as working fluid shows the highest exergy efficiency
 403 (closely followed by the other hydrocarbon mixture and R1233zd(E)). In spite of the lower exergy destruction of the
 404 KC boiler, the higher number of components compared to the ORC leads, on the whole, to higher irreversibility and,
 405 consequently, to a lower second law efficiency. The higher number of components is also responsible for the larger
 406 investment cost of the power plant compared to the ORCs. Furthermore, the power output of the KC is lower than that
 407 of an ORC with R1233zd(E) and it holds the same figures of the hydrocarbon mixtures. For KC and R1233zd(E)
 408 working fluid, the turbine is the component with the highest exergy destruction. On the other hand, for the hydrocarbon
 409 mixtures, the evaporator was found to be the main responsible of the irreversibilities.

410 In the low temperature resource case study (Pomaranca), the KC shows a notably higher efficiency than ORCs (from
 411 22 to 40% depending on the fluid). Differently from the high temperature case study, the optimal ORC working fluid is
 412 R1234ze(Z), which anyhow shows lower performance levels compared to the KC. In particular, the power output of the
 413 ORC is far lower than that achieved with the KC, as well as the first and second law efficiency (by 3 and 15 percentage
 414 points respectively). Differently from the high temperature case study, the higher number of components and thus of
 415 irreversibility sources for the KC is counterbalanced by their better performance, thus achieving, overall, lower
 416 electricity costs compared to ORCs. Like in the high temperature case, the most critical component of KC is the turbine.
 417 On the other hand, for the R1234ze(Z) cycle, the most critical components are the condenser and the evaporator. The
 418 reduced performance of the ORCs also entails an increase of the electricity cost by about 3 c€/kWh when compared to
 419 the KC.

420 **Table 6** Comparison of results of Low- and High- temperature case

	Mt. Amiata case study (212°C)		TLR Pomaranca case study (120°C)	
	KC	ORC (R1233zd(E))	KC	ORC (R1234ze(Z))
Power [kW]	5982	6237	645	483
First law efficiency	0.1684	0.1755	0.1289	0.0966
Second law efficiency	0.5731	0.5943	0.5709	0.4276

Critical component	Turbine	Turbine	Turbine	Condenser; Evaporator
TCI [k€]	8663	8483	2244	1852
Electricity cost	9.125	8.845	12.53	15.53

421

422 The achieved results confirmed that KC is a valuable solution as a binary cycle for the exploitation of low temperature
 423 geothermal resources, whereas in case of high temperature resources ORCs are preferable.

424 The most significant achieved results of the research are the costs of generated electricity by the adoption of binary
 425 power cycles from two deeply different geothermal resources:

- 426 • in the case of high temperature one, power plants in the 6 MW size range showed a cost of electricity
 427 production around 9 c€/kWh, with a modest 3% difference in favour of the best ORC over the KC;
- 428 • in the case of low temperature one, power plants in the 500 kW size range showed costs of electricity between
 429 12 and 15c€/kWh, with a more remarkable difference of about 20% in favour of the KC over the best ORC.
- 430 • High thermodynamic performance were achieved with supercritical CO₂ cycle (which is a step ahead over the
 431 transcritical version) for the low temperature resource, and with hydrocarbon mixtures for the high temperature
 432 resource. However, when considering exergo-economics, their rank falls a bit down, especially for CO₂ cycles.

433 As a concluding remark, we can affirm that the exergo-economic analysis applied to the two case studies of high and
 434 low temperature geothermal resource showed competitive energy production costs of binary cycles in the field of
 435 medium size (5 – 6 MW, Mt. Amiata case) compared to the average national levels for geothermal resources. On the
 436 other hand, in the field of low 500 – 600 kW size, there are no real available data on energy production costs from
 437 geothermal resources. Anyhow, the achieved values of 12 – 15 c€/kWh make them competitive with those of other
 438 renewables in the same size range (*biogas and solid biomass* 17 – 25 c€/kWh, *landfill gas* 5 – 8 c€/kWh, *wind energy*
 439 10 – 16 c€/kWh, *PV* 25 – 35 c€/kWh and *hydro* 18 – 20 c€/kWh, (AEEG, 2013)).

440

441 **References**

442 Arslan, O., “Exergoeconomic evaluation of electricity generation by the medium temperature geothermal resources,
 443 using a Kalina cycle: Simav case study”, in: *International Journal of Thermal Sciences*, Vol. 49, pp. 1866-1873, 2010.

444 Arslan, O., and Yetik, O., “ANN based optimization of supercritical ORC-Binary geothermal power plant: Simav case
445 study”, in: *Applied Thermal Engineering*, Vol. 31, pp. 3922-3928, 2011

446 AEEG Autorità per l’Energia Elettrica, il Gas e il sistema idrico,(2013),*Costi di produzione di energia elettrica da fonti*
447 *rinnovabili*, report2013 by Politecnico di Milano, in Italian.Available at
448 <http://www.autorita.energia.it/allegati/docs/13/RappPolitecnicoRinn.pdf>, last accessed 03 August 2017.

449 Baldacci A., Mannari M., Sansone, F., “Greening of Geothermal Power: An Innovative Technology for Abatement of
450 Hydrogen Sulphide and Mercury Emission”, in: *Proceedings World Geothermal Congress 2005, Antalya, Turkey, 24-*
451 *29 April,2005*.

452 Bayer P., Rybach L., Blum P.H., Brauchler R., “Review of Life Cycle Environmental effects of geothermal power
453 generation”, in: *Renew. Sustain. Energy Rev.*, 26, 446–463, 2013.

454 Bejan, A., Tsatsaronis, G., Moran, M., *Thermal Design and Optimization*, John Wiley & Sons, New York, 1996.

455 Bombarda, P., Invernizzi, C., Pietra, C., “Heat recovery from Diesel engines: A thermodynamic comparison between
456 Kalina and ORC cycles”, in: *Applied Thermal Engineering*, Vol. 30, pp. 212-219, 2009.

457 Bravi M., Basosi R., “Environmental impact of electricity from selected geothermal power plants in Italy”, in: *J. Clean.*
458 *Prod.*, 66, 301–308, 2014.

459 Brown, K., “Antimony and Arsenic Sulfide Scaling in Geothermal Binary Plants”, in: *Proceeding International*
460 *Workshop on Mineral Scaling*, pp. 25-27, 2011.

461 Chemical Engineering, Economic indicators, available at: [https://www.academia.edu/19698484/277921333-CEPCI-](https://www.academia.edu/19698484/277921333-CEPCI-2015)
462 [2015](https://www.academia.edu/19698484/277921333-CEPCI-2015).

463 Dorj, P., “Thermoeconomic Analysis of a New Geothermal Utilization CHP Plant”, in:*Geothermal Training*
464 *Programme*, Reykjavic, Iceland, Vol. 2, p, 74, 2005.

465 Fiaschi, D., Lifshitz, A., Manfrida, G., Tempesti, D., “An innovative ORC power plant layout for heat and power
466 generation from medium to low-temperature geothermal resources”, in: *Energy Conversion and Management*, Vol. 88,
467 pp. 883-893, 2014.

468 Fiaschi, D., Manfrida, G., Talluri, L., “Water-ammonia cycles for the utilization of low temperature geothermal
469 resources”, in: *ASME 2015 Power Conference*, San Diego, United States, 2015.

470 Frick S., Kaltschmitt M., Schorder G., “A Life cycle assessment of geothermal binary power plants using enhanced
471 low-temperature reservoirs”, in: *Energy*, 35, pp. 2281–2294, 2010.

472 Fu, W., Zhu J., Li, T., Zhang, W., Li, J., “Comparison of a Kalina cycle based cascade utilization system with an
473 existing organic Rankine cycle based geothermal power system in an oilfield”, in: *Applied Thermal Engineering*, Vol.
474 58, pp. 224-233, 2013.

475 Ibrahim, M., B., Kovach, R., M., “A Kalina cycle application for power generation”, in: *Energy*, Vol. 18, pp. 961-969,
476 1993.

477 Kalina, I.A., “Generation of energy by means of a working fluid, and regeneration of a working fluid”, *United States*
478 *Patent 434656*. Filed date: Aug. 31,1982.

479 Klein, S.A., Nellis, G.F., *Mastering EES*, f-Chart software, 2012.

480 Klein, S.A., Nellis, G.F., *Thermodynamics*, Cambridge University Press, 2011.

481 Knapek, E., Kittl, G., “Unterhaching Power Plant and Overall System, in: *Proceedings European Geothermal*
482 *Congress*, 2007.

483 Kotas, T.J., *The Exergy Method of Thermal Plant Analysis*, Butterworths, 1985.

484 Leibowitz, H.M., Micak, H.A., “Design of a 2MW Kalina cycle binary module for installation in Husavik, Iceland”, in:
485 *Geothermal Resources Council Transactions*, Vol. 23, pp. 75–80, 1999.

486 Li, S., Dai, Y., “Thermo-economic comparison of Kalina and CO₂ transcritical power cycle for low temperature
487 geothermal sources in China”, in: *Applied Thermal Engineering*, vol. 70 pp. 139-152, 2014.

488 Liu, Q., Duan, Y., Yang, Z., “Effect of condensation temperature glide on the performance of organic Rankine cycles
489 with zeotropic mixture working fluids, in: *Applied Energy*, Vol. 115, pp. 394-404, 2014.

490 Liu, Q., Duan, Y., Yang, Z., “Performance analyses of geothermal organic Rankine cycles with selected hydrocarbon
491 working fluids”, in *Energy*, Vol. 63, pp. 123-132, 2013.

492 Lukawski, M., “Design and Optimization of Standardized Organic Rankine Cycle Power Plant for European
493 Conditions”, University of Akureyri, Master’s thesis, 2009.

494 Mergner, H., Kolbel, T., Schlagermann, P., “Geothermal Power Generation – First Operation Experiences and
495 Performance Analysis of the Kalina Plant in Bruchsal”, in: *Geothermal Power Generation*, 2013.

496 Nag, P., K., Gupta, A. V., “Exergy analysis of the Kalina cycle”, in: *Applied Thermal Engineering*, Vol. 18, pp. 427-
497 439, 1997.

498 Oyewumni, O.A., Kirmse, C.J.W., Pantaleo, A.M., Markides, N., “Performance of working-fluid mixtures in ORC-
499 CHP systems for different heat-demand segments and heat-recovery temperature levels”, in: *Energy Conversion and*
500 *Management*, Vol. 148, pp. 1508-1524, 2017.

501 Rodríguez, C., Palacio, J., Venturini, O., Lora, E., Cobas, V., Santos, D., Dotto, F., Gialluca, V., “Exergetic and
502 economic comparison of ORC and Kalina cycle for low temperature enhanced geothermal system in Brazil”, in:
503 *Applied Thermal Engineering*, Vol.30, pp. 109-119, 2012.

504 Saner D., Juraske R., Kubert M., Blum P., Hellweg S., Bayer P., “*Is it only CO₂ that matters? A life cycle perspective*
505 *on shallow geothermal systems*”, in: *Renew. Sustain. Energy Rev.*, 14, pp. 1798–1813, 2010.

506 Schuster, A., Karellas, S., Kakaras, E., Spliethoff, H., “Energetic and economic investigation of Organic Rankine Cycle
507 applications”, in: *Applied Thermal Engineering*, pp.1809–1817, 2009.

508 Shokati, N., Ranjbar, F., Yari, M., “Exergoeconomic analysis and optimization of basic, dual-pressure and dual-fluid
509 ORCs and Kalina geothermal power plants: A comparative study”, in: *Renewable Energy*, Vol. 83, pp. 527-542, 2015.

510 Szargut, J., Morris, D.R., Steward, F.R., *Exergy analysis of thermal, chemical, and metallurgical processes*,
511 Hemisphere Publishing Corporation, 1988.

512 Turton, R., Bailie, R., Whiting, W., Shaeiwitz, J., *Analysis, Synthesis and Design of Chemical Processes*, Prentice Hall
513 PTR, 2003.

514 Valdimarsson, P., “Factors influencing the economics of the Kalina power cycle and situations of superior
515 performance”, in: *International Geothermal Conference*, pp. 32-40, 2003.

516 Victor, R. A., Kim, J. K., Smith, R., “Composition optimisation of working fluids for Organic Rankine Cycles and
517 Kalina cycles”, in: *Energy*, Vol. 55, pp. 114-126, 2013

518 Walraven, D., Laene, B., D’haeseleer, W., “Economic system optimization of air-cooled organic Rankine cycles
519 powered by low-temperature heat sources”, in: *Energy*, Vol. 80, pp. 104-113, 2015.

520 Yari, M., Mehr A.S., Zare, V., Mahmoudi, S.M.S., Rosen, M.A., “Exergoeconomic comparison of TLC (trilateral
521 Rankine cycle), ORC (organic Rankine cycle) and Kalina cycle using a low grade heat source”, in: *Energy*, vol. 83 pp.
522 712-722, 2015.

523 Zeyghami, M., “Performance analysis and binary working fluid selection of combined flash-binary geothermal cycle”,
524 in: *Energy*, Vol. 88, pp. 76-774, 2015.

525 Zhang, X., He, M., Zhang Y., “A review of research on the Kalina cycle”, in: *Renewable and Sustainable Energy*
526 *Reviews*, Vol. 16, pp. 5309–5318, 2012.

527

528 **Appendix A**

529 The Total Capital Investment (TCI) was evaluated from equation A.1 (Bejan, A., et al., 1996):

$$530 \quad \text{TCI} = \text{FCI} + \text{SUC} + \text{WC} + \text{LRD} \quad \text{A.1}$$

530 Where:

- 531 • FCI = Fixed-Capital Investment
- 532 • SUC= StartUp Costs
- 533 • WC = Working Capital
- 534 • LRD = Costs of Licensing, Research and Development

535 FCI - Fixed-Capital Investment includes direct and indirect costs, which are needed to purchase and install the plant
536 components, as well as the required infrastructure. Direct costs are composed by equipment, material and labour costs;
537 indirect costs derive from the necessary operation for the completion of the powerplant, but will not become part of it.

538 The calculated direct costs, as suggested by (Lukawski, M., 2009), are listed below:

- 539 ▪ Piping, assessed as 7% of PEC;
- 540 ▪ Installation of equipment, which is composed by its transportation, insurance, labour, foundations, working
541 fluid costs and all the other expenses related to a power plant construction. For small geothermal power plants,
542 these costs are estimated to be 6% of PEC;
- 543 ▪ Instrumentation, controls and electrical equipment, which are the electrical equipment costs; in case that the
544 powerplant is near the electricity network, this value can be estimated to be 4% of PEC;
- 545 ▪ Cost of Land –together with civil and structural work, are the “offsite cost”; this cost can be neglected if
546 compared to the other costs;
- 547 ▪ Civil and structural work – assessed as 7% of PEC.

548 The calculated indirect costs, still as suggested by (Lukawski, M., 2009), are listed below:

- 549 ▪ Engineering and supervision – which is composed by planning and design of the plant costs, as well as
550 supervision costs; this cost was estimated to be 6% of PEC;
- 551 ▪ Construction: which is composed by temporary construction cost and contractor’s profit; was assessed as 3%
552 of PEC;

553 ▪ Contingencies: include unexpected events that may occur during transportation or construction of the
554 powerplant. The cost can range between 5% and 20% of FCI, depending on the complexity and peculiarity of
555 the powerplant. The assessed case is a rather standard configuration; therefore the cost was estimated as 8% of
556 FCI.

557 Other TCI costs include:

- 558 ▪ Start Up costs (SUC) – assessed as 1% of FCI.
- 559 ▪ Working capital (WC) – which is the capital invested to cover the operating expenses before financial return
560 derived from the sale of electricity to the grid. It was assumed as 3% of PEC.

561 Geothermal power plants operation and maintenance costs are usually low when compared to the initial investment.
562 They were estimated as 1.5% of the TCI, as suggested by (Schuster, A., et al. 2009).

563 In order to extend the validity of the economic analysis, it is necessary to take into account that money flows occurs at
564 different time periods. Therefore, we actualized these cash flows at a specified year by the following classic
565 relationship:

$$F = P(1 + i_{\text{eff}})^n \quad \text{A.2}$$

566 Where:

- 567 • P is the actualized value of money
- 568 • F is the money value after n years.

569 In order to determine the annual instalment of the TCI, a capital recovery factor, as suggested by Bejan (Bejan, A., et al.
570 1996), was adopted.

$$A = \text{TCI} * \text{CRF} = \text{TCI} * \frac{i_{\text{eff}} \cdot (1 + i_{\text{eff}})^n}{(1 + i_{\text{eff}})^n - 1} \quad \text{A.3}$$

571 Where:

- 572 • CRF – capital recovery factor
- 573 • i_{eff} –effective interest rate = 10%, as suggested by(Dorj, P., 2005)
- 574 • n –power plant lifespan = 20 years

575 The Total powerplant Cost is the sum between the annual instalment of the TCI and the Operation and Maintenance
576 costs (O&M).

$$\text{Total Powerplant Cost} = A + O\&M = TCI * CRF + TCI * 0.015 \quad \text{A.4}$$

577 Assuming the total operating time of the power plants at 7446 h/year (Shokati, N., et al. 2015), for each k-th component,
578 the capital investment was determined.

$$\dot{Z}_k [\text{€}/\text{s}] = \frac{(\text{Total Plant Cost}) * PEC_k}{PEC_{\text{totale}} * 7446 * 3600} \quad \text{A.5}$$

579 The powerplant components exergy destruction cost is defined as the inlet flux costs times the component exergy
580 destruction.

$$\dot{C}_{\text{dis}_k} [\text{€}/\text{s}] = \text{cost}_{\text{fuel}_k} * \dot{E}_{\text{dis}_k} \quad \text{A.6}$$

581 The Total Capital Investment per installed kW was thus defined.

$$TCI_{\text{kW}} \left[\frac{\text{€}}{\text{kW}} \right] = \frac{TCI}{W_t} \quad \text{A.7}$$

582